European Journal of Pharmaceutics and Biopharmaceutics 143 (2019) 91–97

Contents lists available at ScienceDirect

European Journal of Pharmaceutics and Biopharmaceutics

journal homepage: www.elsevier.com/locate/ejpb

Research paper

Occurrence and prevention of Pickering foams in pharmaceutical nano-milling

Róbert Lehocký[a,b], Daniel Pěček[b], Ivan Saloň[a], František Štěpánek[a,*]

[a] Department of Chemical Engineering, University of Chemistry and Technology Prague, Technická 3, Prague 6, 166 28, Czech Republic
[b] Zentiva, k.s., U Kabelovny 130, Praha 10, 102 00, Czech Republic

ARTICLE INFO

Keywords:
Nano-milling
Pickering foam
Nano-suspension
Surfactant
Specific surface area
Stabilisation

ABSTRACT

Particle size reduction to sub-micrometer dimensions in stirred media mills is an increasingly common formulation strategy used for improving the bioavailability of poorly aqueous soluble active pharmaceutical ingredients (APIs). Due to their hydrophobic character, the API particles need to be stabilised by a surfactant in order to form a stable nano-suspension. This work is concerned with the understanding of an undesired phenomenon often encountered during the development and scale-up of wet nano-milling processes for hydrophobic APIs – the formation of foams. We investigate the microstructure, rheology and stability of these foams, and find them to be Pickering foams stabilised by solid particles at the gas-liquid interface rather than by a surfactant. By exploring the effect of surfactant concentration on the on-set of foaming in conjunction with the milling kinetics, we find a relationship between the specific surface area of the nano-suspension, the quantity of surfactant present in the formulation and the occurrence of foaming. We propose a mechanistic explanation of foam formation, and find that in order to prevent foaming, a large surfactant excess of approx. 100x above the critical micelle concentration has to be present in the solution in order to ensure a sufficiently rapid coverage of freshly exposed hydrophobic surfaces formed during the wet nano-milling process.

1. Introduction

The formation of pharmaceutical nano-suspensions by wet milling using stirred media mills is an increasingly common method for improving the bioavailability of poorly water soluble APIs (Active Pharmaceutical Ingredients) [1,2]. By reducing the characteristic particle size to sub-micrometer dimensions, the specific surface area of the API can be increased sufficiently to achieve the desired dissolution rate enhancement even for the thermodynamically most stable crystalline form of the API, without having to search for alternative solid-state forms such as meta-stable polymorphs or amorphs. The chemical engineering principles of stirred media milling are relatively well established [3] based on experience from the processing of materials such as pigments or ceramics. The suspension of particles to be milled is pumped through a mechanically agitated chamber containing milling beads (e.g. stainless steel or zirconia beads), whose impacts result in the fragmentation of the milled material. The nano-miling process is scalable simply by increasing the volume of suspension pumped through the milling chamber. Since the process is closed, it can be operated in a sterile way, enabling the manufacture of novel drug dosage forms such as injectable suspensions for intramuscular depot systems [4]. Due to the predominantly hydrophobic nature of APIs subjected to nano-milling, stabilising agents such as polymers or surfactants have to be added to the formulation in order to ensure colloidal stability and prevent the re-aggregation of the breakage products [2]. Systematic approaches have been proposed to determine feasible composition and process parameters when developing pharmaceutical nano-suspensions [1,5]. However, there are still important challenges associated with the nano-milling process. One of them is the undesired formation of foams, particularly when the process is scaled up from batch to flow-through configuration [5,6]. Foam formation is undesired from the processing point of view because it is associated with a significant increase of viscosity (up to 6 orders ro magnitude), which hinders the flow of the suspension through the milling chamber and also restricts the movement of milling beads in the milling chamber, which ultimately reduces the milling efficiency [20,21]. If the milled product is a nanoparticle suspension intended e.g. for application by injection [4], the formation of a stable foam irreversibly damages the product quality. Therefore, it is important to understand the origin of foaming in pharmaceutical wet nano-milling.

Generally, foams can be stabilised either by surfactants or by solid particles adsorbed at the gas-liquid interface [7–9]. In the latter case

* Corresponding author.
E-mail address: Frantisek.Stepanek@vscht.cz (F. Štěpánek).

https://doi.org/10.1016/j.ejpb.2019.08.016
Received 1 March 2019; Received in revised form 15 August 2019; Accepted 21 August 2019
Available online 22 August 2019
0939-6411/

(the so-called Pickering foams), the increased rigidity of the gas-liquid interface due to the presence of a tightly packed layer of solid particles gives rise to remarkable foam stability and high viscosity. The particle monolayer also acts as a barrier to diffusion across the interface, which not only significantly reduces the rate of liquid evaporation or gas dissolution, but also prevents any solutes present in the liquid phase to adsorb on the particle facets oriented towards the gas phase. For this reason Pickering foams and the so-called armoured bubbles, once formed, are very difficult to de-stabilise by the addition of surfactants to the bulk [10]. In many application areas such as food [11], ceramics [12] or advanced stimuli-responsive materials [13], the high stability and viscosity of Pickering foams are desirable properties. However, in the case of pharmaceutical nano-suspension processing in flow-through stirred media mills, the occurrence of highly viscous and stable foams is strongly undesirable as it prevents efficient recirculation of the suspension through the milling chamber, and reduces the efficiency of contacts between the milling beads and the API particles [20,21]. Therefore, the objectives of the present work were to characterise the properties and microstructure of such foams, to understand the mechanism by which they are formed, and to identify parameters by which foam formation in pharmaceutical wet nano-milling can be suppressed.

2. Materials and methods

2.1. Chemicals

The substance chosen for the milling was a hydrophobic API (kindly donated by Zentiva, k.s.) in the form of dry powder consisting of platelet-like crystals with a characteristic particle size between 5 and 300 μm [4]. It has a very low aqueous solubility (below 0.010 mg/ml). The dispersion medium was particle-free water for injections, which meets pharmacopoeia conditions, containing Tween 20 (polyoxyethylene (20) sorbitan monolaurate, CAS no. 9005-64-5). The API particle concentration in the suspension was fixed at 15.6 % (w/w) and the suspensions were prepared at surfactant/API ratios of 0.038, 0.057, and 0.077 by mass.

2.2. Nano-milling process

The milling process was carried out in a stirred media mill LabStar (Netzsch, Germany) with a 250 ml milling chamber, operated in a closed circulation mode (suspension circulation flowrate 156 g/min) using zirconium dioxide beads (1.0 mm in diameter) at stirring rate of 1000 rpm and ball fill level of 90 % (corresponding to 225 ml of the beads). The batch size was 330 g in all cases. To follow the milling kinetics, samples were collected at predetermined time intervals and subjected to particle size distribution (PSD) analysis by static light scattering and morphology analysis by Scanning Electron Microscopy (SEM).

2.3. Particle size distribution measurement

The particle size distribution (PSD) of the raw material and the suspension at different stages of milling was measured by static light scattering using the Partica LA-950 S2 (Horiba, Japan) in a 230 ml flow cell, using deionised water as the dilution medium. Stirring and sonication was applied. The volume of the injected suspension into the flow cell was in the range of 30 to 250 μl in order to achieve optimum laser attenuation automatically indicated by the instrument. PSD was evaluated by the Fraunhofer kernel and reported on a volume basis.

2.4. Microscopy

The morphology of the crude material as well as the milled, dried suspensions was observed by Scanning Electron Microscopy (SEM, Tescan, Czech Republic). A small volume of the sample was pipetted to a double-sided carbon tape, dried in air, and sputter-coated by gold (Emitech K550X) before imaging. The structure of foams in the wet state was observed by the optical microscope BX41 (Olympus, Japan). The foam sample was placed between two cover-slips and gently pressed; the same area of the foam was imaged at several focal plane positions in order to identify the distribution of API particles relative to the gas-liquid interface. Macroscopic images of the foam were taken by digital camera EOS 100D (Canon, Japan).

2.5. Foam rheology

Rheological characterisation of the foams was performed using a TA Instruments AR-G2 stress-controlled rheometer fitted with a Peltier stage set to 25 °C. All measurements were performed using a 20 mm 2° cone geometry with a gap of 0.500 mm and examined via frequency sweeps (0.01–100 Hz). Data were analysed using the TA Instruments TRIOS software and the apparent viscosity was reported as a function of shear rate.

3. Results and discussion

3.1. Foam occurrence, properties and microstructure

During normal operation of the milling process, the API suspension has a liquid consistency (Fig. 1**a**) and is easily pumped through the milling chamber. However, with an increasing milling time, which is required for achieving the target API particle size in the sub-micron range, the suspension begins to convert into foam. In the early stages of foam formation, the foam can still be pumped through the milling chamber, but eventually the viscosity of the foam becomes so high that the process has to be stopped (Fig. 1**b**). The dynamic viscosity of fully formed foams was in the range of 1–10 kPa·s, and continued to increase with increasing milling time (Fig. 2**a**). For a constant milling time of 60

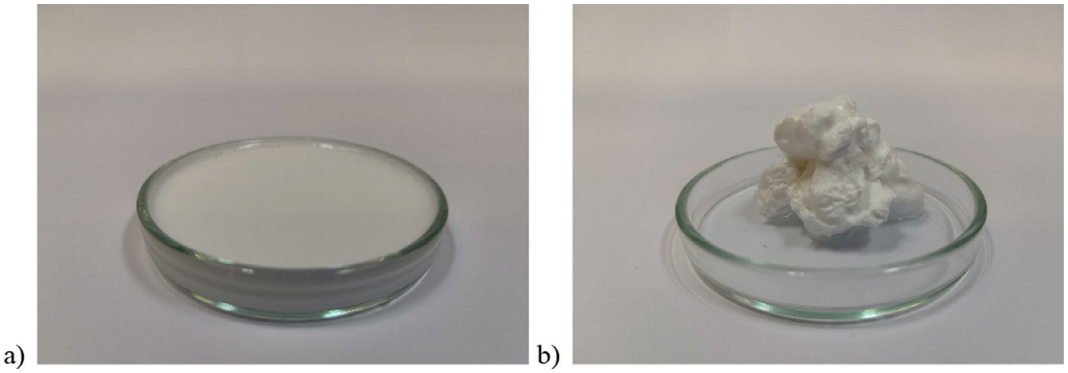

Fig. 1. (a) Aqueous suspension of API particles in the normal state before foam occurrence. (b) Example of a stable foam formed during the wet nano-milling process. The macroscopic composition of the formulation is identical in both cases.

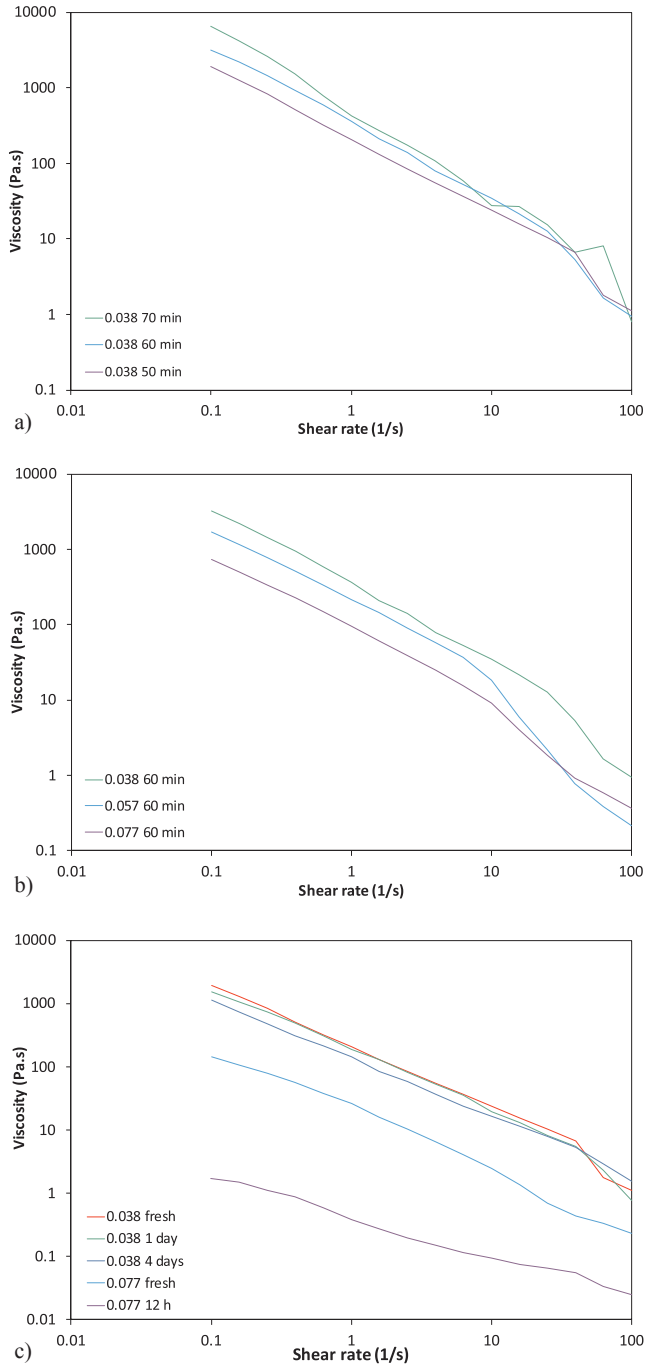

Fig. 2. Rheology of foams. (a) Batch with 0.038 surfactant/API ratio, the apparent viscosity increases with time of the milling. (b) Comparison of batches with different surfactant/API ratios at the same milling time. (c) Effect of surfactant/API ratio on foam stability in time (milling time 50 min for all samples).

min, the foam viscosity was found to depend on the surfactant/API ratio; for higher surfactant/API ratios, slightly less viscous foams were formed, but their viscosity was still in the kPa·s range (Fig. 2**b**), i.e. approximately six orders of magnitude higher than water. The main difference between foams formed at different surfactant/API ratios was their stability. For the purpose of this work we define foam stability as the ability to retain its mechanical (rheological) properties over time, i.e. not to revert back to a liquid form. While foams formed using the highest surfactant/API ratio of 0.077 gradually lost their stability (decrease of dynamic viscosity to approximately 1 Pa·s over 12 h – cf. Fig. 2**c**), foams formed from suspensions with lower surfactant/API ratios were remarkably stable and kept their semi-solid physical consistency for days (Fig. 2**c**). Even after several months of storage in a closed container (to avoid moisture loss by evaporation) at 4 °C (to avoid possible product degradation), there was no sign of liquid drainage or phase separation in the foam.

The fact that the foams were so stable, and that the foam stability increased with decreasing surfactant content in the formulation, suggests that the foams were probably not stabilised by the surfactant, but that a different mechanism might be involved. In “traditional” foams stabilised by surfactant molecules at the gas-liquid interface (e.g. washing-up liquid, shampoo, etc.), a decrease in surfactant concentration generally means reduced foaming. In our system, the trend was opposite. Microscopic analysis of the foam structure in the wet state (Fig. 3**a**) revealed that finely milled API particles were not only dispersed in the bulk aqueous phase, but also present as a mono-layer at the gas-liquid interfaces. This is a characteristic feature of Pickering type dispersions (Pickering emulsions [14], armoured bubbles, particle-stabilised foams, liquid marbles [15]). In this case the foam formation is a way for the newly formed hydrophobic API particles to partially avoid contact with the aqueous phase. A similar mechanism of foaming due to *in situ* formed hydrophobic particles has been reported in the literature for cellulose microparticles [16]. However, in the present case the particles are formed by a purely physical process – milling. The characteristic cell size in the foams was in the range of 10–50 μm (Fig. 3b and c). The fact that formulations with a lower surfactant/API ratio had a tendency to form more rigid foams could be taken as a manifestation of higher gas-liquid interfacial surface area within the foams, caused by a higher number of hydrophobic API particles that prefer to position themselves at the interface.

3.2. Mechanism of foam formation

Based on the finding that the foams are stabilised by particles, a possible mechanism of foam formation can be proposed as shown in Fig. 4. When an API particle is broken up by the impact of milling beads, freshly formed hydrophobic surfaces are exposed. If the aqueous phase locally in contact with these surfaces contains a sufficient concentration of surfactant, the surfactant molecules will adsorb on the newly available surface and the daughter particles will be stabilised in the aqueous phase. In the absence of a sufficient local concentration of surfactant, the next thermodynamically favourable route is for the hydrophobic surfaces to de-wet. This can happen either by partitioning to an existing liquid-gas interface, or by the nucleation and growth of a new bubble. Small air bubbles can be introduced into the circulating suspension in the agitated storage tank. New bubbles can also nucleate directly in the milling chamber from air dissolved in the aqueous phase. Local pressure fluctuation at the point of particle breakage and fragment separation can lead to a cavitation event. A similar mechanism of foam formation by hydrodynamic cavitation in an aqueous suspension of hydrophobic particles (ethyl cellulose) has been reported by Jin et al. [22].

The surfactant concentration in the aqueous phase would appear to be a critical parameter that determines the outcome of the breakage event and ultimately the on-set of foaming. It can be expected that as the surfactant is gradually depleted from the solution by adsorption to newly created hydrophobic surfaces in the course of particle milling, at some point the surfactant concentration will drop below a critical level and foam formation will begin.

3.3. Effect of surfactant on foaming propensity

To verify this mechanism, milling experiments with systematically varying surfactant/API ratios under otherwise identical conditions were carried out and the particle size distribution (PSD) was measured as function of time (Fig. 5). The on-set of foaming was recorded in each case, and the experiment was stopped when a fully developed foam

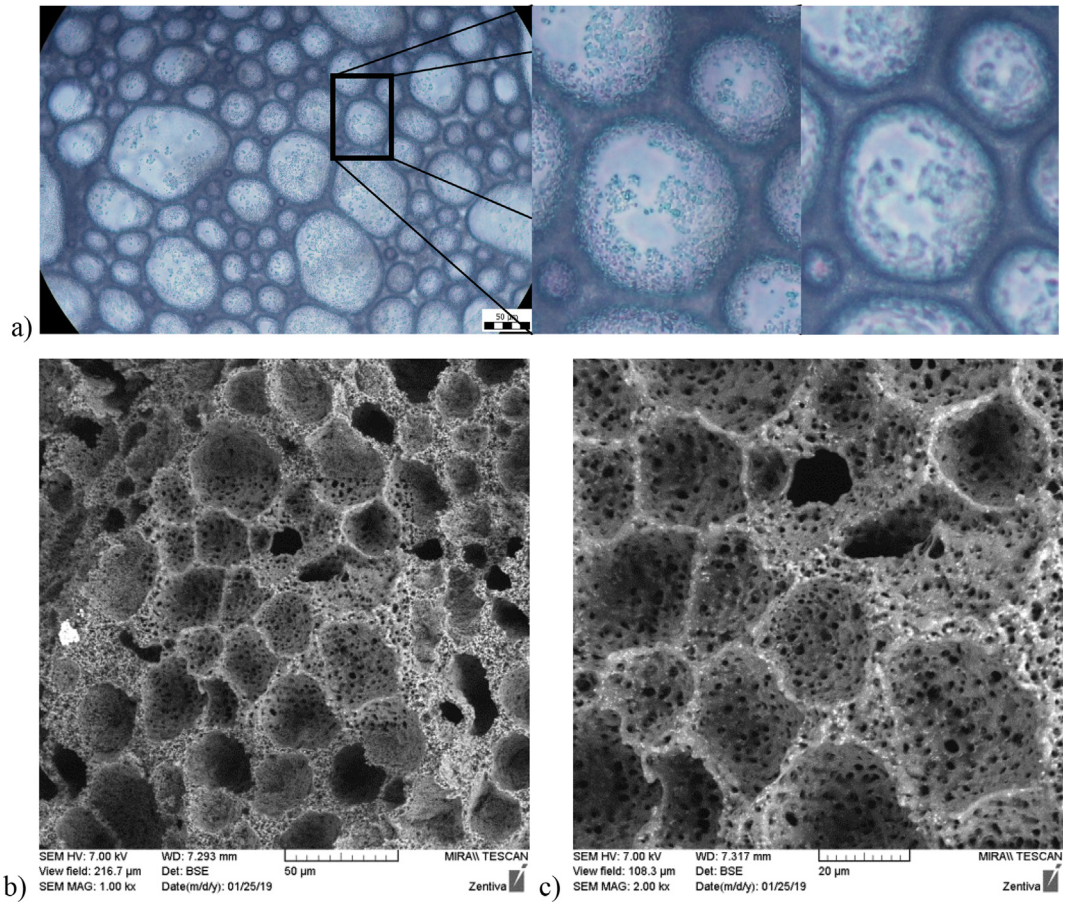

Fig. 3. (a) Optical microscopy of foam structure; the magnified view at different focal planes shows the distribution of particles at the gas-liquid interface. (b), (c) SEM micrographs of dry foam showing its cellular structure.

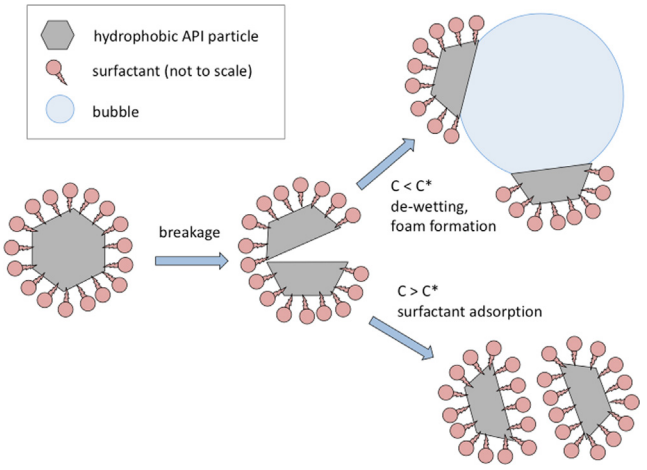

Fig. 4. Proposed mechanism of foam formation. Hydrophobic surfaces freshly exposed after particle break-up can be stabilised either by surfactant adsorption if sufficient surfactant excess is locally available, or by de-wetting and partitioning at the gas-liquid interface.

occurred. Although the API solubility slightly increases with surfactant concentration (0.026 mg/ml in a 1% (w/w) aqueous solution of Tween 20), the quantity of API dissolved is still so low that it does not affect the overall solids fraction in the suspension. Specifically, the dissolved API represents no more than approx. 0.014 % of the solid API even in the case of the highest surfactant/API ratio used. As shown in Fig. 5, the initial stages of the breakage kinetics are rather similar irrespective of the surfactant/API ratio: within the first 5 min the raw material with a relatively broad size distribution between 10 µm and 100 µm is milled down to a monomodal PSD positioned between 1 µm and 10 µm, from which a growing peak of approximately 200 nm particles is then gradually formed. Note that the shoulders apparent in the initial PSD at t = 0 min in Fig. 5a and c were due to weak particle aggregates present in the raw API; the initial PSD of the primary particles are otherwise identical, as evidenced by the curves at t = 5 min where any initial aggregates are already dispersed.

What distinguishes the three cases with different surfactant/API ratios is the extent to which the sub-micron particles have formed before giving rise to foaming. For the lowest surfactant/API ratio of 0.038, the sub-micron fraction represents only about 17 % by volume at the time of foam formation, whereas for the highest surfactant/API ratio of 0.077 almost 89 % of the particles by volume were in the sub-micron range before the foam started to form. The increasing proportion of sub-micron particles can also be seen qualitatively on SEM micrographs of milled material recovered from the suspensions at the on-set of foaming and shown in Fig. 6.

The decreasing API particle size is associated with an increase of the specific surface area, which can be calculated from the PSD according to

$$s_{API} = \frac{6}{d_{3,2}\,\rho_{API}} \tag{1}$$

where $d_{3,2}$ is the Sauter mean diameter evaluated from the PSD and ρ_{API} is the material density of the API (1.2 g/cm^3). The progress of the milling experiments in terms of the specific surface area is plotted in Fig. 7, along with the time at which the on-set of foaming was first detected in each case. It is evident that the on-set of foaming can be delayed by increasing the quantity of surfactant in the formulation: for

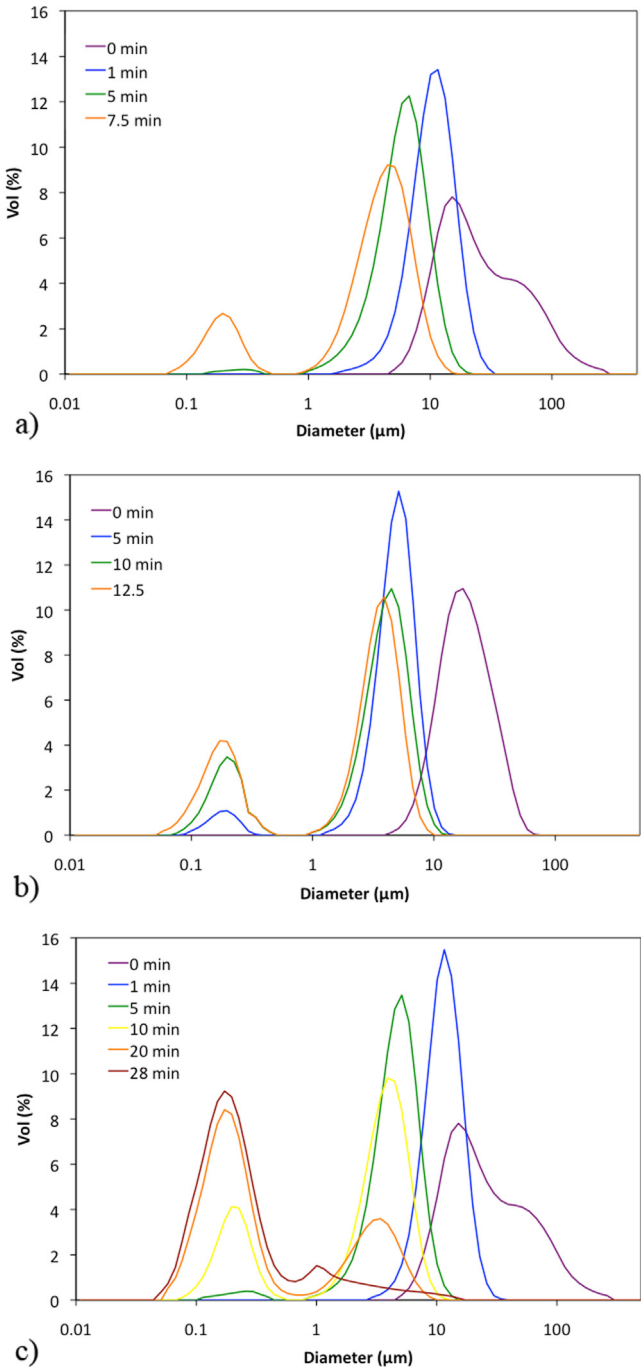

Fig. 5. Evolution of particle size distribution during wet nano-milling at different surfactant/API ratios; (a) 0.038; (b) 0.057; (c) 0.077.

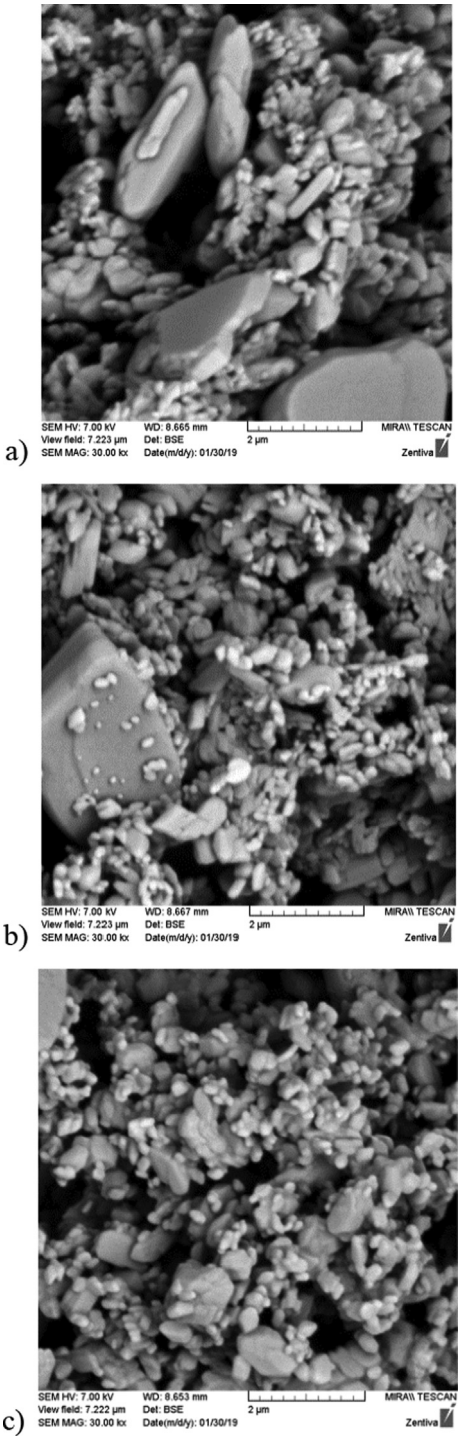

Fig. 6. SEM micrographs of API particles at different stages of milling; (a) 0.038 surfactant/API ratio and 7.5 min; (b) 0.057 surfactant/API ratio and 12.5 min; (c) 0.077 surfactant/API ratio and 25 min of milling. The scale bar represents 2 µm.

surfactant/API mass ratio of 0.038, 0.057 and 0.077, foaming first occurred at 6 min, 13 min and 24 min, respectively. The API specific surface area corresponding to these time points was approx. 3 m^2/g, 12 m^2/g, and 27 m^2/g, respectively (Fig. 7). Note that all three cases follow the same milling curve due to the fact that identical milling conditions (mill RPM, bead size, bead fill level, etc.) were used. The so-called breakage limit for these conditions appears to have been reached for milling times approaching 30 min, as indicated by the plateau in Fig. 7 and the invariable peak around 200 nm in Fig. 5.

By considering the topological polar surface area of Tween 20 approx. 1.33 nm^2 [17,18], the theoretical quantity of surfactant required for covering the particle surface can be estimated and compared with the actual quantity of surfactant present in the system. This comparison is shown in Fig. 8, which clearly demonstrates a direct proportionality between the surfactant/API ratio and the particle surface area at which foaming began. Interestingly, this analysis also reveals that a significant (but remarkably constant) excess of surfactant is required if foaming is to be avoided. The surfactant concentration in the aqueous phase at the on-set of foaming was calculated from the difference between the actual and the theoretically required quantity of surfactant according to the formula

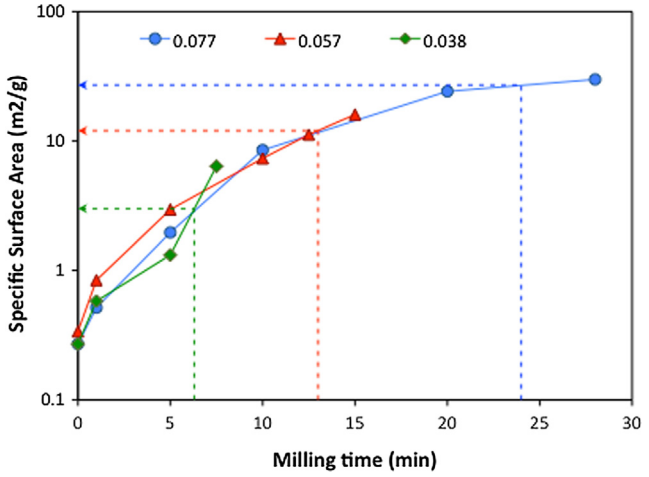

Fig. 7. Milling kinetics expressed as the evolution of API specific surface area calculated from the measured particle size distributions at each time point for different surfactant/API ratios as indicated in the legend. The dashed lines denote the on-set of foaming in each case.

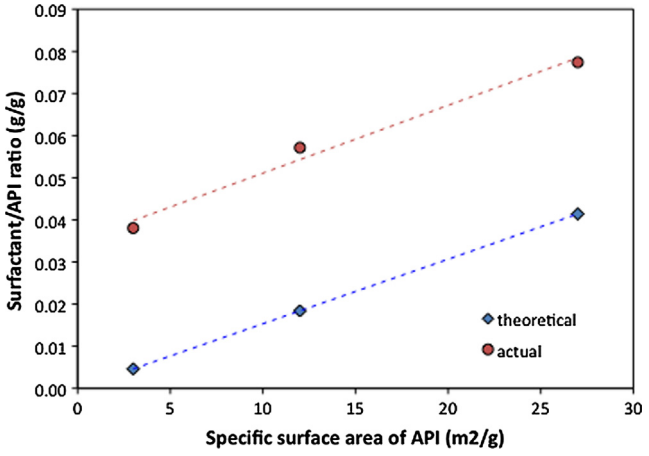

Fig. 8. Theoretical surfactant/API ratio required for covering a given surface area of the API particles, compared with the actual surfactant/API ratio at the on-set of foaming.

$$c_{surf} = \frac{1}{V}\left(\frac{m_{surf}}{M_{w,surf}} - \frac{m_{API}\ s_{API}}{a_{0,surf}\ N_A}\right) \quad (2)$$

where V is the volume of water, m_{surf} is the total mass of surfactant in the formulation, $M_{w,surf}$ is the molar weight of the surfactant, m_{API} and s_{API} is the mass and the specific surface area of the API, respectively, $a_{0,surf}$ is the polar head area of the surfactant and N_A is the Avogadro's constant. From the experimental data, the mean surfactant concentration at the on-set of foaming was 5.46 ± 0.38 mM (6.71 ± 0.48 g/l). This is approximately 100 times higher than the critical micelle concentration (CMC) of Tween 20 (approx. 0.06 mM at room temperature [19]). Such large surfactant excess can be explained by referring back to the mechanism shown in Fig. 4 and considering that the individual particle breakage is an extremely rapid event. It can be hypothesised that in order to avoid foaming, the surfactant required for covering the freshly exposed hydrophobic surfaces must be immediately present in a local volume element of the aqueous phase that first comes into contact with the daughter particle. If there is not enough surfactant locally and additional surfactant would need to diffuse from the bulk, then surface de-wetting and bubble formation become the more likely scenario (Fig. 4) and the Pickering foam begins to form.

4. Conclusions

This work was concerned with understanding the origins of foam formation during wet nano-milling of hydrophobic pharmaceutical substances in a stirred media mill. Analysis of the foam structure revealed that fine drug particles were present at the liquid-gas interface, stabilising the foam by a Pickering mechanism. The foams were found to be remarkably stable due to lack of diffusive access to the hydrophobic particle facets from the bulk liquid phase. This is undesirable from the processing point of view: once the foam is fully formed in a flow-through stirred media mill, there is no way back and the process has to be stopped. The on-set of foam formation was shown to be directly related with the specific surface area of the API particles and with the free surfactant concentration in the formulation. A mechanism of foam formation has been proposed based on micro-scale events occurring during particle breakage – in order to re-wet freshly exposed hydrophobic surfaces formed by particle breakage and stabilise the particle in the suspension, a local excess of surfactant had to be present. Otherwise the particle tends to de-wet or position itself at an existing liquid-gas interface and contribute to foam formation. From the practical point of view, the knowledge that approximately 100x excess of surfactant relative to its CMC is required in order to avoid foaming can be taken as a basis for pharmaceutical formulation development. When designing wet nano-milling processes for hydrophobic APIs, the specific surface area s_{API} should be calculated from the target PSD of the nanosuspension, the theoretical surfactant quantity estimated from the head area of the surfactant considered for API stabilisation, and then the actual quantity of surfactant m_{surf} calculated from the required volume of the suspension using Eq. (2) such that the necessary surfactant excess c_{surf} be present. From the kinetics point of view, it could be hypothesised that lower M_w surfactants with the ability to adsorb more rapidly to the newly formed hydrophobic surfaces might not require so high surfactant access and still be able to prevent foaming. Alternatively, reducing the rate at which new hydrophobic surfaces are formed *in situ*, i.e. operation the wet milling process under less aggressive conditions (e.g. lower RPM in the milling chamber) might also be a way of suppressing the occurrence of Pickering foams in pharmaceutical nano-milling.

Acknowledgments

We would like to thank Zentiva, k.s., for kindly providing materials and granting access to equipment used in this work. F.Š. would like to acknowledge funding from the Czech Science Foundation (GAČR project no. 19-26127X). R.L. would like to acknowledge support from the Specific University Research (MŠMT project no. 21-SVV/2018).

References

[1] M. Li, M. Azad, R. Davé, E. Bilgili, Nanomilling of drugs for bioavailability enhancement: a holistic formulation-process perspective, Pharmaceutics 8 (2016) 17.
[2] L. Peltonen, J. Hirvonen, Pharmaceutical nanocrystals by nanomilling: critical process parameters, particle fracturing and stabilization methods, J. Pharm. Pharmacol. 62 (2010) 1569–1579.
[3] F. Stenger, S. Mende, J. Schwedes, W. Peukert, Nanomilling in stirred media mills, Chem. Eng. Sci. 60 (2005) 4557–4565.
[4] R. Lehocký, D. Pěček, F. Štěpánek, Scale-up from batch to flow-through wet milling process for injectable depot formulation, Eur. J. Pharm. Sci. 95 (2016) 122–129.
[5] M. Juhnke, J. Berghausen, C. Timpe, Accelerated formulation development for nanomilled active pharmaceutical ingredients using a screening approach, Chem. Eng. Technol. 33 (2010) 1412–1418.
[6] A. Bitterlich, C. Laabs, E. Busmann, A. Grandeury, M. Juhnke, H. Bunjes, A. Kwade, Challenges in nanogrinding of active pharmaceutical ingredients, Chem. Eng. Technol. 37 (2014) 840–846.
[7] B.P. Binks, M. Kirkland, J.A. Rodrigues, Origin of stabilisation of aqueous foams in nanoparticle–surfactant mixtures, Soft Matter 4 (2008) 2373–2382.
[8] A. Cervantes Martinez, E. Rio, G. Delon, A. Saint-Jalmes, D. Langevin, B.P. Binks, On the origin of the remarkable stability of aqueous foams stabilised by nanoparticles: link with microscopic surface properties, Soft Matter 4 (2008) 1531–1535.
[9] U.T. Gonzenbach, A.R. Studart, E. Tervoort, L.J. Gauckler, Stabilization of foams with inorganic colloidal particles, Langmuir 22 (2006) 10983–10988.

[10] A.B. Subramaniam, C. Mejean, M. Abkarian, H.A. Stone, Microstructure, morphology, and lifetime of armored bubbles exposed to surfactants, Langmuir 22 (2006) 5986–5990.
[11] E. Dickinson, Food emulsions and foams: Stabilization by particles, Curr. Opin. Colloid Interf. Sci. 15 (2010) 40–49.
[12] A.R. Studart, U.T. Gonzenbach, E. Tervoort, L.J. Gauckler, Processing routes to macroporous ceramics: a review, J. Am. Ceram. Soc. 89 (2006) 1771–1789.
[13] S. Fujii, Y. Nakamura, Stimuli-responsive bubbles and foams stabilized with solid particles, Langmuir 33 (2017) 7365–7379.
[14] J. Čejková, J. Hanuš, F. Štěpánek, Investigation of internal microstructure and thermo-responsive properties of composite PNIPAM/silica microcapsules, J. Colloid Interf. Sci. 346 (2010) 352–360.
[15] P. Janská, O. Rychecký, A. Zadražil, F. Štěpánek, J. Čejková, Liquid oil marbles: increasing the bio-availability of poorly water-soluble drugs, J. Pharm. Sci. 108 (2019) 2136–2142.
[16] H.A. Wege, S. Kim, V.N. Paunov, Q. Zhong, O.D. Velev, Long-term stabilization of foams and emulsions with in-situ formed microparticles from hydrophobic cellulose, Langmuir 24 (2008) 9245–9253.
[17] W. Zhu, P. Sabatino, R. Govoreanu, K. Verbruggen, J.C. Martins, P. Van der Meeren, Preferential adsorption of polysorbate 20 molecular species in aqueous paliperidone palmitate suspensions, Colloids Surf., A 384 (2011) 691–697.
[18] National Center for Biotechnology Information. PubChem Compound Database; CID = 443314, < https://pubchem.ncbi.nlm.nih.gov/compound/443314 > (accessed Jan. 31, 2019).
[19] K.L. Mittal, Determination of CMC of polysorbate 20 in aqueous solution by surface tension method, J. Pharm. Sci. 61 (1972) 1334–1335.
[20] S. Ouattara, C. Frances, Grinding of calcite suspensions in a stirred media mill: effect of operational parameters on the product quality and the specific energy, Powder Technol. 255 (2014) 89–97.
[21] C. Knieke, S. Romeis, W. Peukert, Influence of process parameters on breakage kinetics and grinding limit at the nanoscale, AIChE J. 57 (2011) 1751–1758.
[22] H. Jin, W. Zhou, J. Cao, S.D. Stoyanov, T.B.J. Blijdenstein, P.W.N. de Groot, L.N. Arnaudov, E.G. Pelan, Super stable foams stabilized by colloidal ethyl cellulose particles, Soft Matter 8 (2012) 2194–2205.